

Tomographic Fracture Imaging (TFI): Direct 5D Mapping of Transmissive Fracture/fault Zones Using Seismic Emission Tomography (SET)

Peter Geiser and Peter Leary

Global Microseismic Services, 1625 Broadway, Denver, Colorado 80202

peter.geiser@globalgeophysical.com

Keywords: Tomographic Imaging; Permeability Field

ABSTRACT

TFI is a proven method for direct 4D mapping of transmissive fracture/fault networks with over 50 successful projects completed for the Oil and Gas industry. TFI uses Seismic Emission Tomography (SET) to capture the weak but spatially and temporally coherent seismic emissions of hydraulically transmissive fracture/fault damage zones. TFI works by utilizing two phenomena of the Earth's brittle crust.

1. The near critical state where stress changes as low as or lower than 0.01 bar are associated with failure on pre-existing fractures.
2. Fluid pressure (Pf) waves due to changes in Pf that propagate through transmissive networks for distances that can be at the kilometer scale and at velocities of 10s of meters/second.

TFI differs from conventional microearthquake passive seismic techniques in two ways:

1. TFI can extract objective images of the actual fracture/fault surfaces, thus eliminating the need for the more subjective interpretation of hypo-central clouds.
2. It uses stacking rather than standard hypo-central location techniques.

Stacking from seconds to hours allows the weak signal of the fracture damage zone seismicity to emerge from the noise. TFI has proven X,Y accuracy of as much as one voxel, with a typical cubic voxel size of 8 m (25 ft) on an edge. In all cases (>20) where independent evidence for the location of transmissive fracture/faults existed, TFI locations were confirmed. We give the geological and geophysical framework for TFI. As an example of TFI we show a movie sequence of 1 minute intervals during which a Pf wave induced by a frac moved along a natural transmissive fairway to intersect a 2nd well over 700 m from the treatment well. The Pf wave preceded the arrival of the fluid in the well intersected by the fairway by 2 stages.

1. INTRODUCTION

A major problem for accessing both geothermal energy and hydrocarbon resources is accurate imaging the permeability field architecture. To date, this has largely been done by indirect methods e.g. 3D seismic attributes, shear wave splitting and microseismic hypocentral techniques. While these indirect techniques can be integrated to provide an independent check the results still ultimately require subjective interpretation (e.g. Williams-Stroud et al, 2012, Mueller, M., 2013). Tomographic Fracture Imaging (Geiser et al, 2012) uses seismic emission tomography (Geiser et al, 2006) to directly image the fractures, thereby removing the subjectivity inherent in the indirect methods. TFI is distinct from other methods that use tomographic seismic techniques. These methods e.g. Duncan and Lakings (2006), Markatis, et al (2012) use SET to locate "proxy" hypo-centers from which the fracture/fault locations must be inferred. In contrast TFI data acquisition and processing are based on empirical data on the nature of fracture systems (Geiser et al, 2006, 2012) and the critical state of the Earths brittle crust (Leary, 1997; Zoback, 2007). This fundamental difference in the physical basis of processing the seismic data i.e. TFI processing algorithms are based on the actual behavior of fracture/fault zones vs. hypo-central location techniques based on trigonometry and seismic wave physics. Thus fracture data imaged with TFI are objective compared to the subjective ones resulting from interpreting the hypo-central clouds either by hand or statistically.

An outline of the physical basis of the seismic data processing for TFI is as follows:

1. The critical behavior of the Earth's brittle crust and the known dislocation like slip on faults e.g. Elliott,D. (1976), Lockner et al (1991) form the basis for processing the seismic data as semblance.
2. Processing of the continuously recorded seismic data uses a field, and experiment-based empirical model of fracturing/faulting in which the physical discontinuity is surrounded by a damage zone where the fracture density increases follows a power law as the discontinuity is approached (Geiser et al, 2006, 2012). Figure 1 shows an example of a damage zone and its relationship to the physical discontinuity imaged as a TFI.

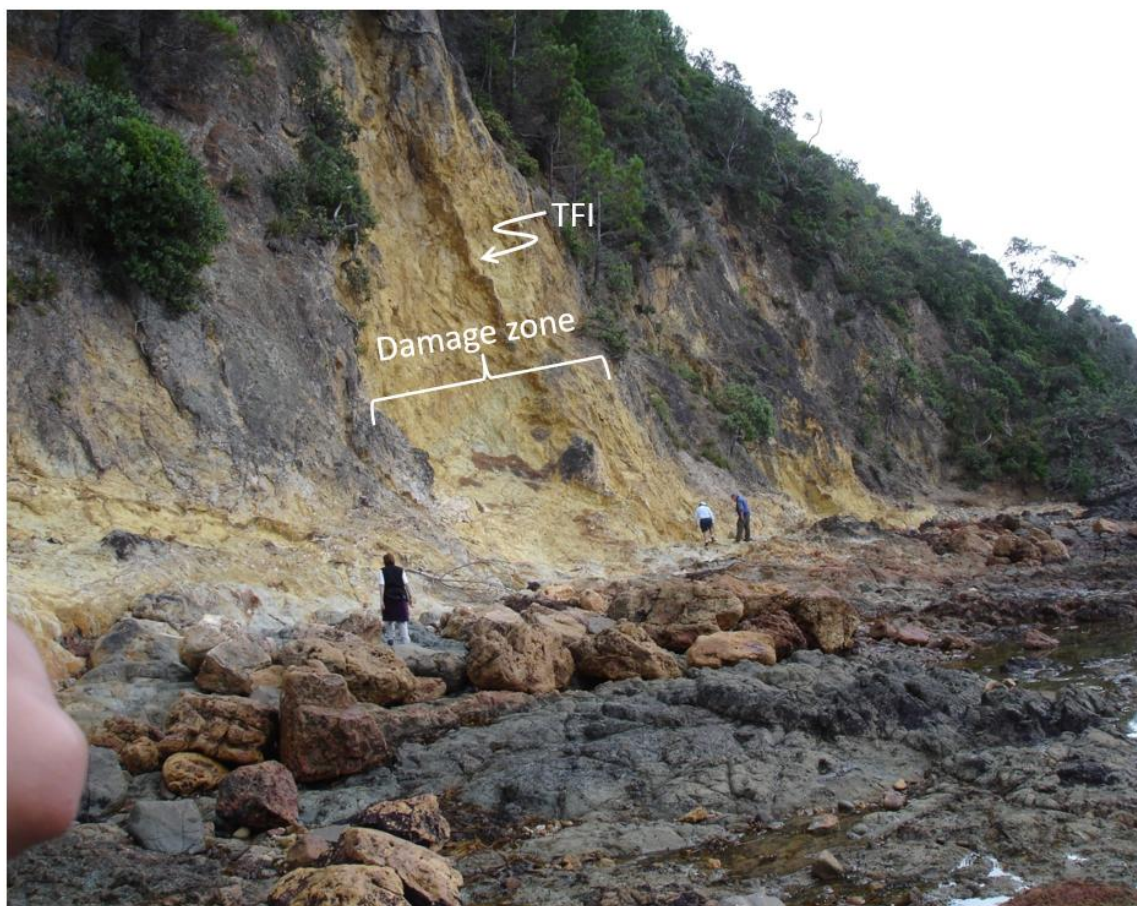


Figure 1: Outcrop of greywacke of Coromandel Formation, New Zealand showing relationship of damage zone to physical discontinuity of a transmissive fracture labeled as a TFI. TFIs are images of the physical discontinuity embedded in the damage zone.

3. The very low strength of the brittle crust (Ziv and Rubin, 2000) means that very small stress perturbations (< 0.01 bar) such as those produced by Earth tides can produce failure on pre-existing fractures. This implies that the Earth's brittle crust is in a constant state of failure at the grain scale.
4. The weak signal of this continual failure, cannot be captured by standard micro-earthquake techniques. However because the damage zones are regions of very high crack density that emit seismic energy over times lasting for seconds to hours from fixed geographic loci, the signal can be extracted from the noise by stacking. These methods are more fully described in Geiser et al (2006, 2012), Sicking et al (2013), and Lacazette et al (2013).

Of particular relevance for this discussion is the abundant evidence for the presence of what Geiser et al. (2006, 2012) have inferred to be fluid pressure (Pf) waves generated by small fluctuations in Pf induced by fracturing or production. Evidence for this phenomenon was first noted by Heffer et al. (1995) and was captured by Geiser et al (2006) in the Barnett. Additional data on the Pf wave was recorded at the MAL 145 wells (Geiser et al, 2012). The Pf wave moves through the transmissive fracture network. Because of the very low crustal strength, it causes pre-existing fracture to fail thereby illuminating the fracture/fault fairways. The Barnett and MAL 145 data show that the Pf wave velocity is on the order of tens of meters/sec and can excite fractures kilometers from the source.

2. ILLUMINATION OF A TRANSMISSIVE FRACTURE SYSTEM DURING A FRAC: A MARCELLUS EXAMPLE.

All rock contains two types of mechanical weakness, pre-existing fractures and pre-existing directions of mechanical weakness sometimes referred to as tectonic "fabric" e.g, Turner and Weiss, 1957; Geiser and Engelder, 1983; Engelder and Geiser, 1984. The former are pre-existing fracture/fault zones and the latter control the directions of the induced fracturing generated by fracturing. These directions of mechanical weakness reflect tectonic fabrics imposed during the rock history. In order to induce fracturing, fluid pressures must reach values that are somewhat greater than the minimum horizontal stress (Sh_{min}). Once this pressure is achieved (the "breakdown" pressure), the rock responds by failing along the pre-existing joints and/or along the tectonic fabric directions.

The following set of images show the variation in the behavior of fracturing induced by a hydraulic frac. The activity is captured using semblance as a proxy for the seismic energy emitted by the failure of fractures activated by both seismic waves generated by fracture propagation as well as that induced by Pf waves created by the hydraulic fracturing. The figures show a sequence of map slices through the semblance volume at the well depth. Each slice is from a 10 minute stacked volume of semblance data. The set of images are data selected from the approximately 2.3 hours of a frac stage. In this example, the stage 3 frac intersected a pre-existing transmissive fracture zone linked to an adjacent well. The fracture was intersected again during stage 5. During this

stage a pressure pulse and fluid from this stage was identified in the monitor well. The TFIs coincide with the stage and perf locations, the two independent data on the fluid (pressure and tracer) confirm that the TFI intersected in Stage 5 is transmissive. While we have no independent data supporting the actual path of the fracture the following supports the fracture geometry shown;

1. The fracture intersects the well at the stage locations,
2. It is in fluid contact with the well,
3. Circular histograms of TFI segment orientations correspond to known joint directions.

Figure 2 is a map slice at the well depth showing the Stage 3 TFI of this fracture zone and its relationship to the lateral.

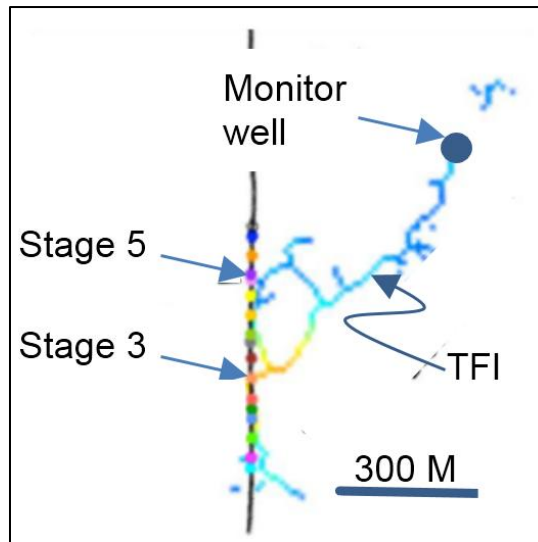


Figure 2: Map slice at well depth showing relationship of Stage 3 TFI of transmissive fracture zone to stages in frac. Colored filled circles on well show perf locations. Colors of TFI show relative semblance values with yellow high and blue low.

2.1 Well Depth Map Slices Through Semblance Volumes Showing Seismic Energy Activity During a Frac.

Figure 3 shows well log data for the bottom hole pressure (BHP) and slurry rate for the initial Pf build up leading to formation breakdown with a Pcrit of about 11,500 psi. These data show that Pf was less than Pcrit for a period of about 17 minutes.

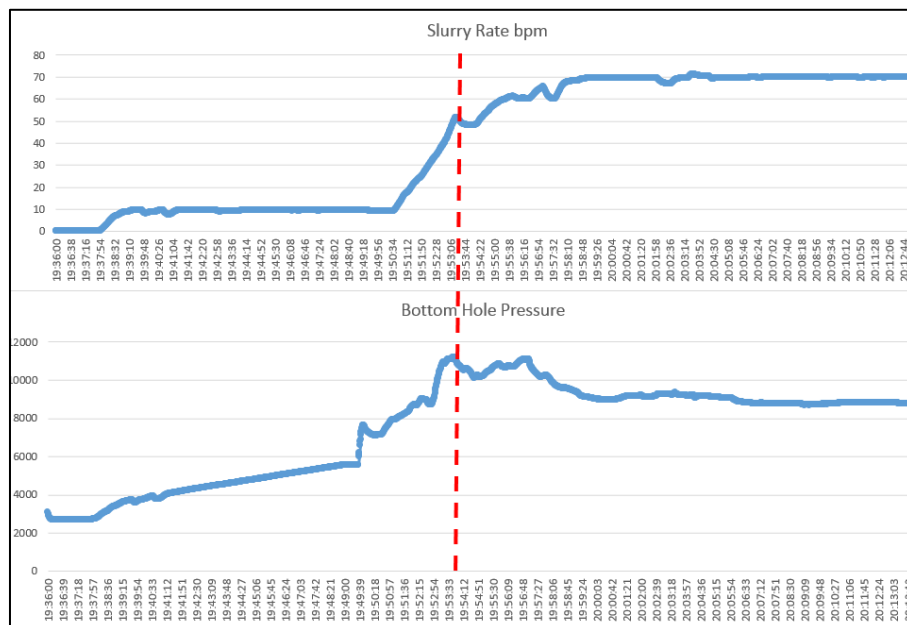


Figure 3: Stage 3 Well log data of initial fluid pressure build up and Slurry rate. Dashed red line shows the time of formation breakdown.

2.2 $P_f < SH_{min}$;

Figure 4 shows the semblance data for the initial fluid pressure build up during the first 14 minutes of the frac prior to reaching breakdown pressure. Consistent with evidence for the very weak critical nature of the crust, these data show that activity on the transmissive fracture is initiated well before the breakdown pressure is achieved. The velocity of the P_f wave is on the order of 10 m/sec. The gap in the band of high semblance connecting the stage 3 frac and the observation well, may be due to any of the following:

1. Out of plane connectivity;
2. A portion of the fracture that is either weaker than the parts that are illuminated thus emitting less seismic energy and therefore below the noise floor of the processing;
3. Portions of the fracture zone that are open fluid conduits

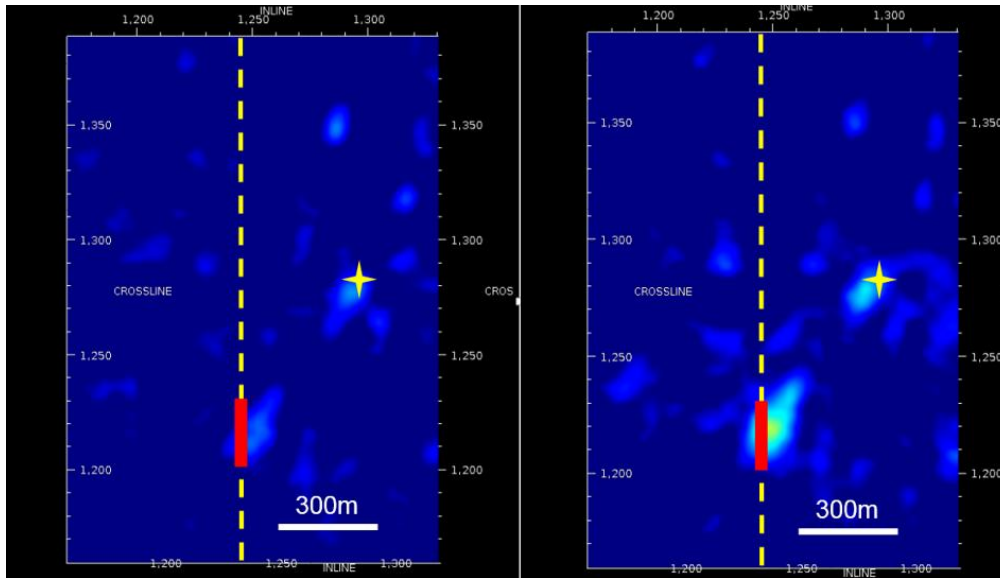


Figure 4: Map slices through Semblance volume at well depth during about the first 14 minutes of frac. Note that weak activity in the damage zone of the transmissive fracture connecting the stage to the observation well has begun along the location of the TFL. The red bar shows the location of stage 3. The yellow star locates the observation well. Left image is approximately 3 minutes after frac inception. Right image is approximately 14 minutes after inception.

2.3 $P_f = SH_{min}$

TFI semblance data show that failure activity induced by fracing follows the “Earthquake cycle” of stress build up and relaxation. Figure 5 shows the activity at or near the time of formation break down and the gradual dying away of activity over a period of about 16 minutes as the strain energy is relaxed. Note that the bloom of energy around the stage contrasts to the more linear semblance bands which characterize the location of transmissive fracture zones. The “bloom” is interpreted as largely reflecting the activation of grain scale failure due to the seismic energy released by the induced fractures rather than activation by a P_f wave.

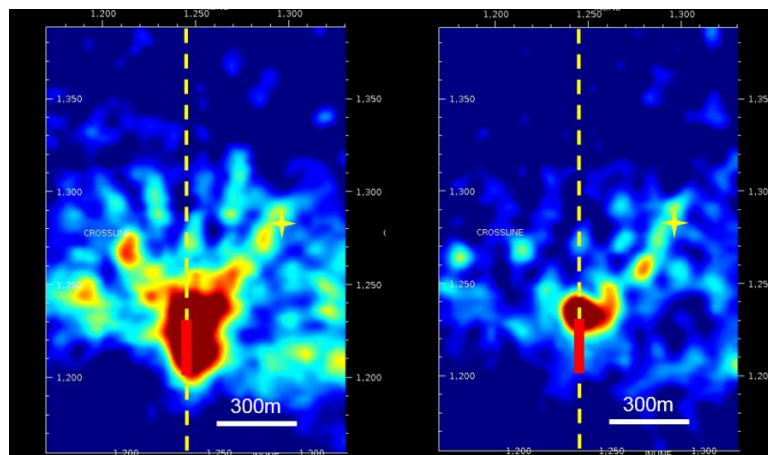


Figure 5: Left image shows frac at breakdown pressure approximately 17 minutes after frac initiation. Right image approximately 55 minutes after frac initiation. Although breakdown pressure is maintained failure activity diminishes as strain energy is depleted by brittle failure.

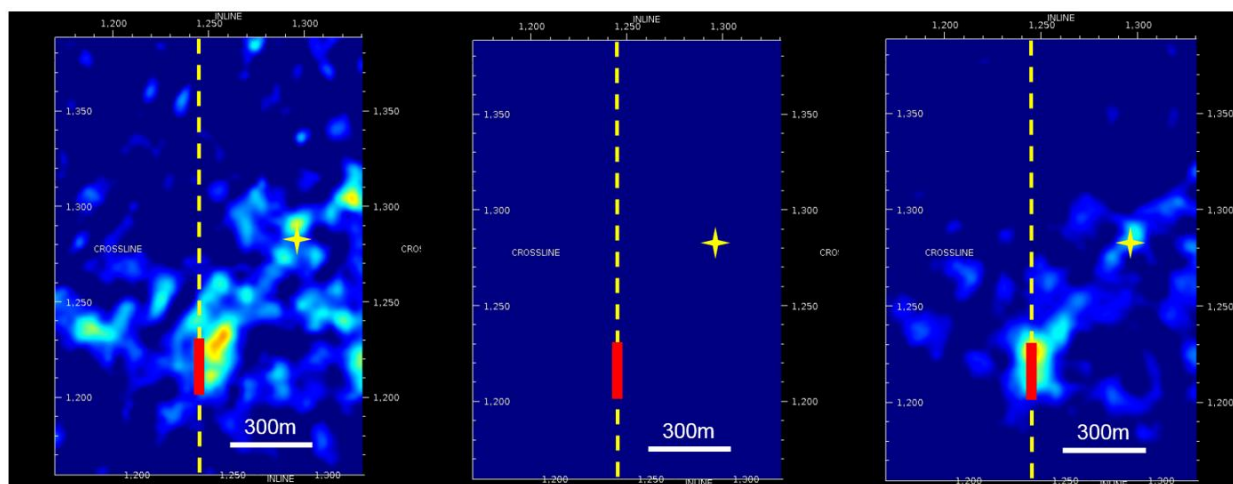


Figure 6: Map slices of semblance volume showing complete sequence of the “earthquake cycle” of stress build up and relaxation. Left image is approximately 80 minutes following frac initiation. Center image is at about 96 minutes and right image is at about 120 minutes.

In the left image semblance energy is diminishing until at about 96 minutes there is insufficient strain energy in the rock to continue fracture activity. By about 120 minutes activity is again increasing as strain energy begins to build. Fluid pressure is maintained at the “breakdown” level throughout the sequence but results primarily in re-activation of activity on the initially perturbed fractures but in little if any additional fracturing.

3. CONCLUSIONS

We have presented data showing that changes in Pf can be used to illuminate the transmissive fracture/fault networks of reservoir permeability fields. These networks have lateral and vertical dimensions at the kilometer scale. We note that in addition to the independent pressure and tracer data supporting the interpretation that these networks are fluid conduits, under continuous Pf loading by hydraulic fracturing, the networks show behavior of stress build up and relaxation, similar to the “earthquake” cycle. Stress cycling, a known characteristic of earthquake faults, is inferred to further support the interpretation of the TFI as fracture/fault zones. Finally we conclude that continuous recording of seismic data for SET when processed using methods based on empirically derived models of the physical behavior of the Earth’s brittle crust can objectively and accurately image the transmissive fracture networks of the permeability field. These data show that it is now possible to overcome one of the major barriers to the successful exploitation of the geothermal resource, namely lack of accurate information on the permeability field.

REFERENCES

- Duncan, P. and Lakings, J.: Frontier Exploration using passive seismic. EAGE Passive Seismic Workshop, Dubai, United Arab Emirates, extended Abstracts, A22 (2006).
- Elliott, D.: The energy balance and deformation mechanisms of thrust sheets, *Phil. Trans. R. Soc. London, A*, **283**, (1976), 289-312.
- Engelder, T. and Geiser, P.: Residual stress in the Tully Limestone, Appalachian Plateau, New York. *J. Geophys. Res.*, **89**, (1984), 9365-9370
- Geiser, P.A. and Engelder, T.: The distribution of layer parallel shortening fabrics in the Appalachian foreland of New York and Pennsylvania: evidence for two non-coaxial phases of the Alleghenian orogeny. In: Hatcher, R., Williams, H., and Zeitz, I. (eds.), *The Tectonics and Geophysics of Mountain Ranges*. *Geol. Soc. Amer. Mem.* 158, (1983), 161-175.
- Geiser, P. A., Vermilye, J., Scammell, R. and Roecker, S.: Seismic used to directly map reservoir permeability fields. *Oil & Gas Journal*, Dec. 11, Dec. 18 (2006).
- Geiser, P., Lacazette, A. and Vermilye, J.: Beyond “dots in a box”, *First Break*, **30**, (2012), 63 – 69.
- Lacazette, A., Vermilye, J., Fereja, S., Sicking, C.: Ambient fracture imaging: A new passive seismic method: SPE 168849 / URTeC 1582380, 10p. (2013).
- Leary P.C.: Rock as a critical-point system and the inherent implausibility of reliable earthquake prediction: *Geophysical Journal International*, **131**, (1997), 451-466.
- Lockner, D. A., Byerlee, J. D., Kuksenko, V., Ponomarev, A., and Sidorini, A.: Quasi-static fault growth and shear fracture energy in granite. *Nature* **350**: (1991), 39-42.
- Markatis, N., Polychronopoulou, K. and Tselentis, G.: Passive seismic tomography: a passive concept actively evolving, *First Break*, **30**, (2012), 83-90.
- Mueller, M.: Meeting the challenge of uncertainty in surface micro-seismic monitoring, *First Break*, **31**, (2013), 89-93.

- Sicking, C., Vermilye, J., Geiser, P., Lacazette, A.: Permeability field imaging from microseismic. *Geophysical Society of Houston Journal*, 3 March, (2013), 11-13.
- Turner, F. J. and Weiss, L. E.: *Structural Analysis of metamorphic tectonites*, McGraw-Hill Book Company, 545 p. (1963).
- Williams-Stroud, S.C., Barker, W. B. and Smith, K.L: Modelling the response of natural fracture networks to induced hydraulic fractures in stimulation treatments, *First Break*, **30**, (2012), 71-75.
- Ziv, A. and Rubin, A. M.: Static stress transfer and earthquake triggering: No lower threshold in sight?, *J. Geophys. Res.*, **105** (B6), (2000), 13631-13642.
- Zoback, M.D.: *Reservoir Geomechanics*. Cambridge University Press, 464 pp. (2007)